Article:
Eisele, H. and Kamoua, R. (2004) Submillimeter-wave InP Gunn devices. IEEE Transactions on Microwave Theory and Techniques, 52 (10). pp. 2371-2378. ISSN 0018-9480

http://dx.doi.org/10.1109/TMTT.2004.835974

Submillimeter-Wave InP Gunn Devices

Heribert Eisele, *Senior Member, IEEE,* and Ridha Kamoua, *Member, IEEE*

***Abstract*—Recent advances in design and technology significantly improved the performance of low-noise InP Gunn devices in oscillators first at D-band (110–170 GHz) and then at W-band (75–110 GHz) frequencies. More importantly, they next resulted in orders of magnitude higher RF output power levels above D-band and operation in a second-harmonic mode up to at least 325 GHz. Examples of the state-of-the-art performance are continuous-wave RF power levels of more than 30 mW at 193 GHz, more than 3.5 mW at 300 GHz, and more than 2 mW at 315 GHz. The dc power requirements of these oscillators compare favorably with those of RF sources driving frequency multiplier chains to reach the same output RF power levels and frequencies. Two different types of doping profiles, a graded profile and one with a doping notch at the cathode, are prime candidates for operation at submillimeter-wave frequencies. Generation of significant RF power levels from InP Gunn devices with these optimized doping profiles is predicted up to at least 500 GHz and the performance predictions for the two different types of doping profiles are compared.**

***Index Terms*—Gunn devices, millimeter-wave devices, millimeter-wave generation, millimeter-wave oscillators, oscillator noise, phase noise, submillimeter-wave devices, submillimeter-wave generation, submillimeter-wave oscillators.**

I. Introduction

EMERGING systems applications at terahertz frequencies, such as imaging, chemical, or biological sensing, and wide-bandwidth communications, require compact, reliable, efficient, and low-noise RF sources as transmitters or local oscillators (LOs) [1]. GaAs and InP transferred-electron devices (TEDs), also called Gunn devices, have been utilized as low-noise RF sources up to millimeter-wave frequencies since their inception over three decades ago. Basic material properties were thought to impose fundamental frequency limits on GaAs and InP TEDs of approximately 100 and 200 GHz, respectively [2]–[4]. As can be seen from the results of Fig. 1, under continuous-wave (CW) operation, experimental data over a wide frequency range appeared to confirm those early predictions. However, recent theoretical and experimental work on fundamental-mode operation at D-band (110–170 GHz) frequencies [5], [6] indicated that optimized device structures and much improved heat dissipation extend the operation of Gunn devices, in particular, of InP devices, to much higher frequencies. These studies also identified RF power extraction at the second or higher harmonic frequencies as a very efficient method of reaching submillimeter-wave frequencies [7], [8].

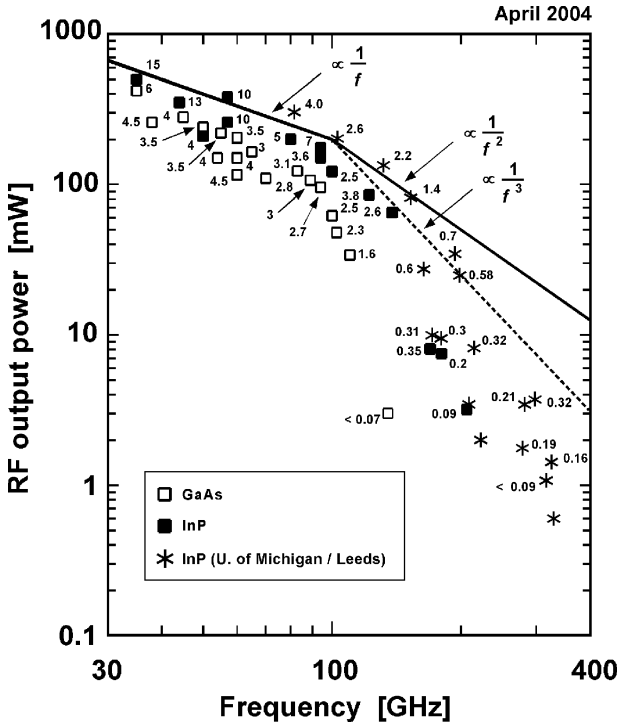

Fig. 1. State-of-the art results from GaAs and InP Gunn devices under CW operation in the 30–400-GHz frequency range. Numbers next to the symbols denote dc-to-RF conversion efficiencies in percent.

This paper reviews the recent major improvements in measured performance mainly at G-band (140–220 GHz) and J-band (220–325 GHz) frequencies and then compares the performance predictions for two types of doping profiles that are prime candidates for operation in a second-harmonic mode at even higher submillimeter-wave frequencies. These simulations took the measured performance into account to improve the accuracy of the predictions and to avoid any overestimation of the inherent frequency limits of Gunn devices.

II. Measured Performance of InP Gunn Devices

A. G-Band Performance

Second-harmonic power extraction was initially investigated with devices whose graded doping profile, as shown in Fig. 2(a), was designed for fundamental-mode operation at D-band frequencies [5], [6]. As can be seen from Fig. 1, devices from this epitaxial material yielded state-of-the-art performance both at D- and J-band frequencies [7], [9]. Likewise, devices on diamond heat sinks whose graded doping profile, as shown

Manuscript received April 30, 2003. This work was supported in part by the National Science Foundation under Grant ECS 98-03781, by the Jet Propulsion Laboratory under Contract 961299 and Contract 961527, and by the Air Force Office of Scientific Research under Contract F49620-00-1-0328.

H. Eisele was with the Solid-State Electronics Laboratory, Department of Electrical Engineering and Computer Science, The University of Michigan at Ann Arbor, Ann Arbor, MI 48109-2122 USA. He is now with the Institute of Microwaves and Photonics, School of Electronic and Electrical Engineering, The University of Leeds, Leeds LS2 9JT, U.K. (e-mail: h.eisele@leeds.ac.uk).

R. Kamoua is with the Department of Electrical and Computer Engineering, State University of New York at Stony Brook, Stony Brook, NY 11794-2350 USA (e-mail: ridha@ece.sunysb.edu).

Digital Object Identifier 10.1109/TMTT.2004.835974

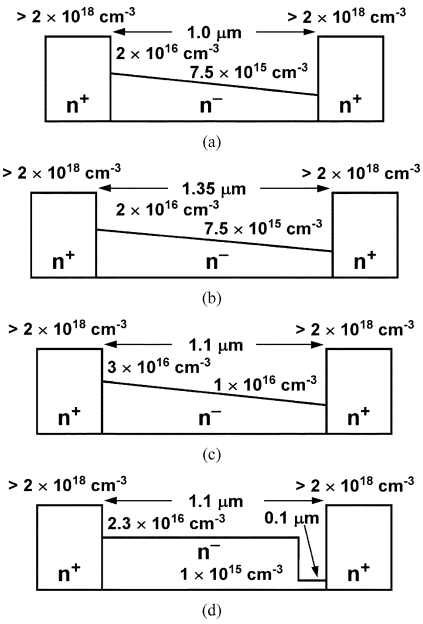

Fig. 2. Nominal doping profiles of InP Gunn devices evaluated for second-harmonic power extraction at G- and J-band.

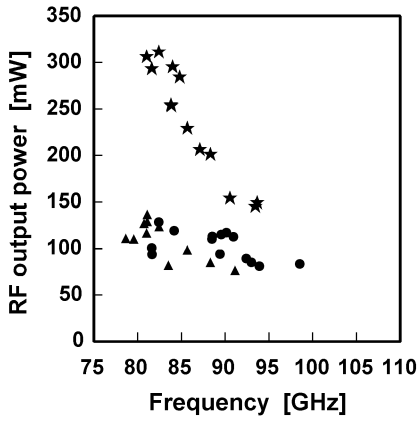

Fig. 3. Performance of fundamental-mode InP Gunn devices with nominal doping profiles of Fig. 2(b) in the 75–100-GHz frequency range. ● ▲: devices on integral heat sinks. ⋆: devices on diamond heat sinks.

in Fig. 2(b), was designed for fundamental-mode operation at W-band (75–110 GHz) frequencies, also generated the highest RF power levels from any Gunn device. Fig. 3 summarizes the results from these devices on diamond heat sinks, but also compares them with those from devices on integral heat sinks. The best result, which is also shown in Fig. 1, was the RF power of 310 mW and the corresponding dc-to-RF conversion efficiency of more than 4% at the oscillation frequency of 82.4 GHz [10].

As a consequence of this performance in the fundamental mode, devices from the same epitaxial material, but with smaller diameters, were evaluated for second-harmonic power extraction at G-band. The waveguide cavity, shown in Fig. 4, is a scaled version of the Carlstrom design [11] and was employed previously in similar experiments [12], [13] with devices that had a nearly flat doping profile and integral heat sinks [14]. Devices also on integral heat sinks, but with the graded doping profiles, were tested in the frequency range of 150–210 GHz and yielded much improved RF power levels of 10 and 9.5 mW at

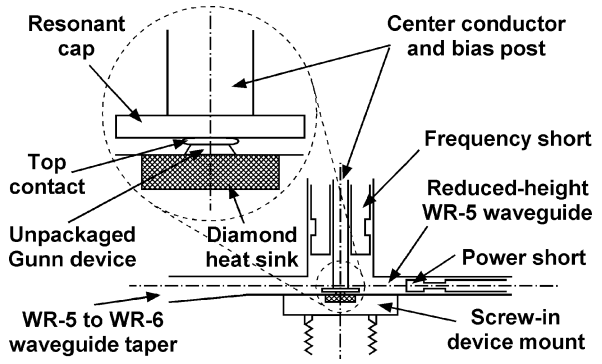

Fig. 4. Schematic of the WR-5/6 waveguide cavity for second-harmonic power extraction at G-band (140–220 GHz).

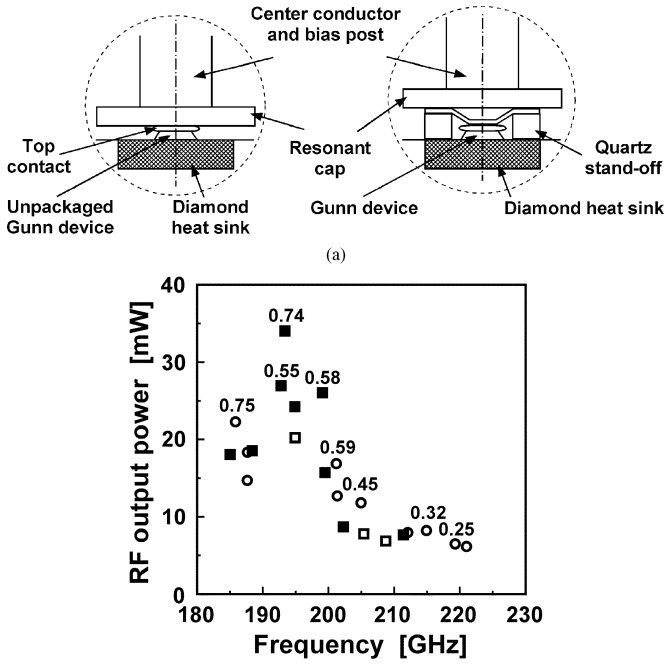

Fig. 5. (a) Schematic cross section of the configuration of an unpackaged and a packaged Gunn device in the waveguide cavity of Fig. 4, dimensions not to scale. (b) RF performance of packaged (◯) and unpackaged (■) InP Gunn devices on diamond heat sinks in a second-harmonic mode in the 180–230-GHz frequency range.

171.5 and 179.8 GHz, respectively [15]. Devices with the same graded doping profiles, but on diamond heat sinks, were also tested in the frequency range of 150–210 GHz, but with a resonant cap diameter of 0.90 mm. They generated more than three times the RF output power compared to devices on integral heat sinks. This improvement is attributed not only to much lower heat-flow resistances of devices on diamond heat sinks, but also to the more favorable distance between the resonant cap and the bottom of the waveguide [16]. The resonant cap also makes direct contact with the electroplated top contact of the device, which eliminates the generally negative influence of package parasitics.

Fig. 5 summarizes the best performance of devices on diamond heat sinks, which occurred at higher oscillation frequencies of around 195 GHz compared to devices on integral heat sinks. The highest RF output power (and corresponding

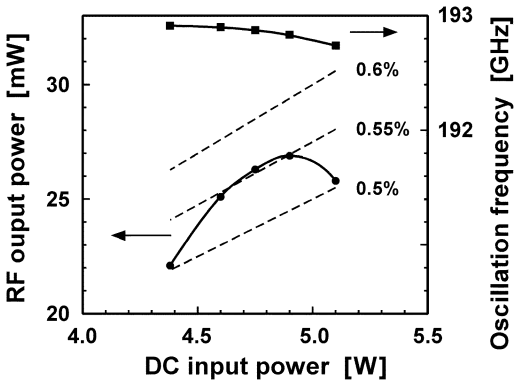

Fig. 6. Bias-dependent RF characteristics of a G-band InP Gunn device in a second-harmonic mode. •: RF output power, ■: oscillation frequency, − − −: lines of constant dc-to-RF conversion efficiency.

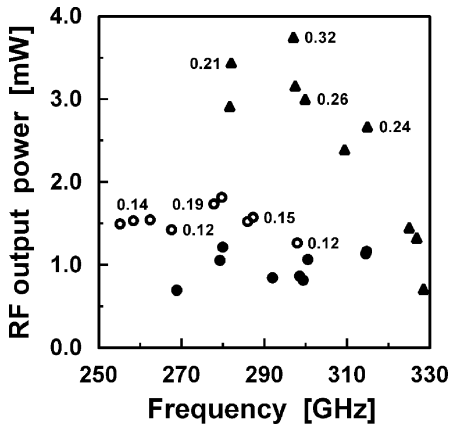

Fig. 7. RF performance of InP Gunn devices on diamond heat sinks operating in a second-harmonic mode in the 250–330-GHz frequency range. •; and ◯: doping profile of Fig. 2(a); ▲: doping profile of Fig. 2(c).

dc-to-RF conversion efficiency) of 34 mW (0.74%) was measured at 193.4 GHz.

For systems applications, devices in a rugged package are preferred. Therefore, devices in an open package with four quartz standoffs and tapered leads were also evaluated. As can be seen from Fig. 5(a), the distance from the resonant cap to the bottom of the waveguide is higher than that without the package and the feed point is different as well. Therefore, the impedance levels at the feed point of the resonant cap are higher and, consequently, smaller device areas must be chosen. Fig. 5(b) summarizes the first set of results from this still ongoing performance comparison. These results clearly indicate that the dc-to-RF conversion efficiencies are not affected by this type of package and that the lower RF output power level can be largely attributed to the smaller area of a packaged device. As also can be seen from Fig. 5(b), the RF power is reduced by less than 3 dB if at all. Due to their smaller size and, consequently, smaller capacitance, the packaged devices reach higher operating frequencies of up to 222 GHz.

The spectra of the free-running oscillators were recorded at select intermediate RF power levels and all power levels of Fig. 5(b). A phase noise of -94 dBc/Hz was determined at 500 kHz off the carrier for a device generating the RF output power of 19 mW at 193.1 GHz [16]. This phase noise represents a typical value and is at the noise floor of the employed spectrum analyzer and harmonic mixer. Therefore, the actual phase noise was estimated to be at least 3 dB lower and correctly reflected the excellent noise performance of devices in fundamental-mode operation from the same epitaxial material [10].

Fig. 6 shows the bias-dependent RF characteristics of one device when the frequency and power shorts of the oscillator were first tuned for maximum RF output power and then kept fixed. The oscillation frequency was tuned electronically by more than 200 MHz, which is sufficient for phase locking. Over this tuning range, the RF output power changed by less than 1 dB [16].

B. J-Band Performance

The aforementioned second-harmonic power extraction from D-band InP Gunn devices on diamond heat sinks yielded RF power levels of typically more than 1 mW up to 315 GHz [7],

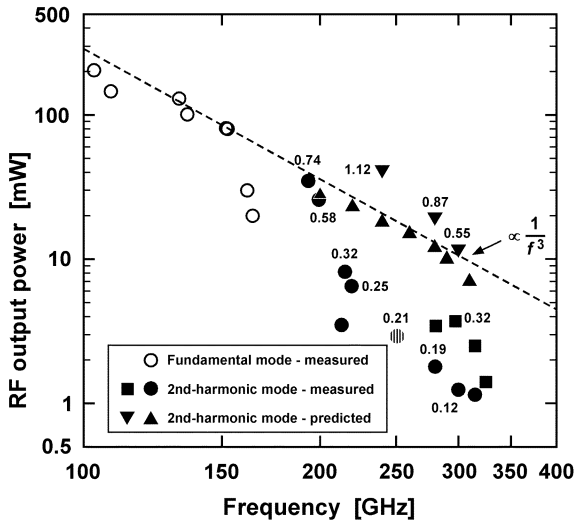

Fig. 8. Comparison of predicted and measured CW RF power levels from InP Gunn devices on diamond heat sinks with an $n^+n^-n^+$ structure and a doping gradient in the active region for the 100-400-GHz frequency range. ◯, •, and ▲ denote structures with doping profiles for both fundamental and second-harmonic mode operation including those of Fig. 2(a) and (b). ■ and ▼ denote a structure with the doping profile of Fig. 2(c).

which already constituted the most powerful solid-state fundamental oscillator operated at room temperature. Fig. 7 summarizes the best results from these devices. In an ongoing effort, these results and those from devices in fundamental-mode operation at W- and D-band frequencies were and are being compared with predictions from an ensemble Monte Carlo harmonic-balance (MCHB) device simulation program [8], [17]. This computer program and its predictions for submillimeter-wave frequencies are discussed in a subsequent section.

As can be seen from Fig. 8, excellent agreement was found between measurements and predictions for the same or very similar graded doping profiles of devices with operating frequencies up to 200 GHz. Predictions for fundamental-mode operation at W- and D-band frequencies are indicated in Fig. 8 by the trend line. The discrepancy between the measured and predicted performance in Fig. 8 at 210–220 GHz is attributed mainly to the smaller areas of packaged devices, as already discussed in Section II-A. The discrepancy of a factor of up to six

at 250–315 GHz is attributed to: 1) slight differences between the actual doping profiles and those assumed in the simulations; 2) package parasitics that affect the performance more significantly at higher oscillation frequencies; and 3) the employed waveguide circuit [7]. This waveguide circuit is less optimized for second-harmonic power extraction than that of Fig. 4 and, for reasons similar to those for packaged devices of Fig. 5, its use with devices packaged with four quartz standoffs requires smaller device areas than assumed under optimum conditions in the simulations. More work is required to account for all relevant causes of these discrepancies and to improve the agreement between predictions and measurements even further.

Subsequently, the MCHB simulation program was employed to optimize doping profiles for second-harmonic power extraction at J-band frequencies. Fig. 2(c) and (d) shows two of those profiles [10] for RF power generation at a target frequency of 240 GHz.

Devices with the doping profile of Fig. 2(c) were first evaluated in the 260–320-GHz frequency range in a waveguide circuit similar to that of [7], and these initial results are included in Fig. 7. Although the devices were operated at frequencies significantly above the target frequency of 240 GHz, their RF output power levels and corresponding dc-to-RF conversion efficiencies more than doubled between 280–315 GHz compared to devices with the doping profile of Fig. 2(a). The highest RF output power of 3.7 mW and the corresponding dc-to-RF conversion efficiency of 0.32% were measured at 297.1 GHz. Operation in a second-harmonic mode was confirmed up to at least 328 GHz in a similar way, as in previous experiments [9]. It should be noted that the discrepancy between measured and predicted RF power levels is now less than a factor of three around 300 GHz, whereas measured and predicted dc-to-RF conversion efficiencies agree within less than a factor of two.

C. Comparison With Other Solid-State CW RF Sources

Impact avalanche transit-time (IMPATT) diodes are still the most powerful fundamental solid-state RF sources at millimeter-wave frequencies [18], [19]. Fig. 9 summarizes published state-of-the-art results from IMPATT and other transit-time diodes. A comparison of the best results of Figs. 7 and 9 shows that, above 290 GHz, InP Gunn devices outperform even Si IMPATT diodes [20] and are the most powerful fundamental solid-state RF sources operated at room temperature.

The most common approach to RF power generation above D-band frequencies employs frequency multipliers with GaAs Schottky-barrier varactor or heterojunction-barrier varactor (HBV) diodes that are driven by RF sources at medium millimeter-wave frequencies of typically 60–100 GHz [1], [21]. Fig. 10 compares the state-of-the-art results from frequency multipliers or frequency-multiplier chains with those from InP Gunn devices, tunnel injection transit-time (TUNNETT) diodes, and resonant tunneling diodes (RTDs). It should be noted here that some of the highest RF power levels were generated by frequency multipliers with arrays of 2–6 Schottky-barrier diodes for increased power-handling capabilities and power-combined RF sources for increased input power [1]. Therefore, the results from InP Gunn devices without the use of power combining compare quite favorably.

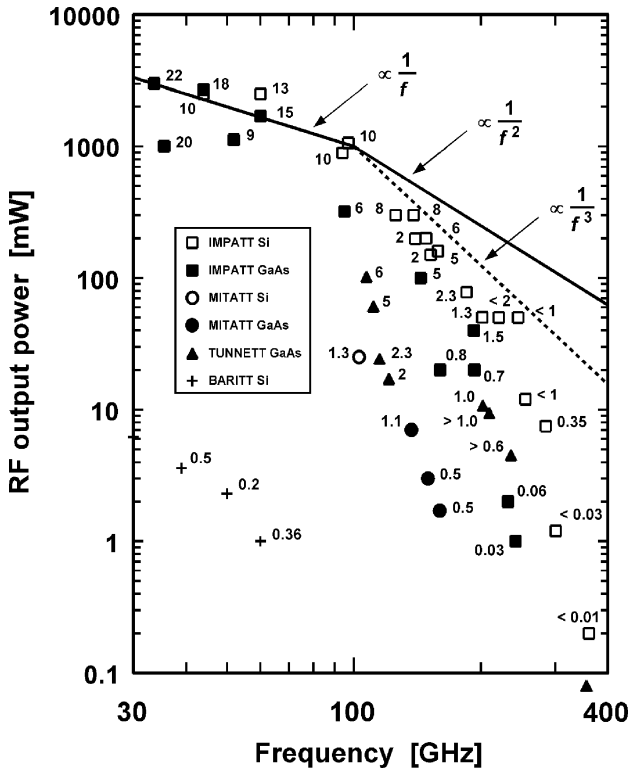

Fig. 9. Published state-of-the art results from Si and GaAs transit-time diodes under CW operation in the 30–400-GHz frequency range. Numbers next to the symbols denote dc-to-RF conversion efficiencies in percent.

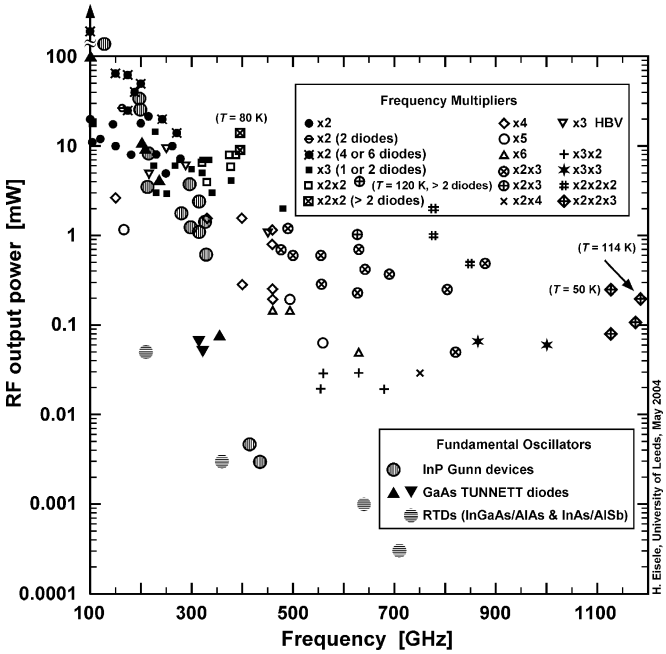

Fig. 10. Published state-of-the-art results from frequency multipliers with GaAs Schottky-barrier varactor diodes or InP-based HBV diodes in the 100–1200-GHz frequency range in comparison with published state-of-the-art results from GaAs TUNNETT diodes, InP Gunn devices, and RTDs above 200 GHz. Frequency multipliers and fundamental oscillators were all operated at room temperature, except where noted.

More importantly, the dc power consumption of the best oscillator each of Figs. 5 and 7 at 193 and 298 GHz is below 4.5 and 1.2 W, respectively. These values compare quite favorably

with those of RF sources that drive frequency multipliers of similar RF output power levels and output frequencies, as shown in Fig. 10. The low dc power consumption also corresponds to low active-layer temperatures in these devices on diamond heat sinks. They were estimated to be typically much below 150 °C, which ensures reliable long-term operation. In addition, the dc power consumption of the best devices of Fig. 7 is in the range of 1.2–1.6 W, which allows operation from a battery. It is expected to decrease even further with oscillator optimization.

More recently, photomixing in fast photodiodes has been exploited extensively to generate RF power at high millimeter- and submillimeter-wave frequencies [22]–[24] since this approach offers higher instantaneous tuning and power generation bandwidths than those of many other solid-state sources. However, even the most powerful sources with InP-based uni-traveling-carrier (UTC) photodiodes [25] generate much less RF output power and require much more dc input power for the laser diodes and optical erbium-doped fiber amplifiers than the Gunn devices of Figs. 5 and 7. It should also be noted that these photodiodes and Gunn devices share two physical properties that significantly limit the power generating capabilities of all known electronic devices at submillimeter-wave frequencies, which are: 1) the relevant carrier drift velocities, i.e., the electron drift velocity in Gunn devices and UTC photodiodes, which forces the use of shorter device lengths at higher operating frequencies and 2) the device capacitance, which, in turn, increases as the device length shrinks and makes impedance matching to the load circuit more and more difficult, the higher its value and the higher the fundamental frequency. A detailed unified analysis, however, is not within the scope of this paper. One possible solution to this problem in oscillators with two-terminal devices is the optimized extraction of higher harmonics, which is currently being investigated [25].

III. Predicted Gunn-Device Performance

Hydrodynamic or energy-momentum device models were applied initially to Gunn devices up to lower millimeter-wave frequencies, where the average effect from different electron scattering mechanisms describes relevant device properties with sufficient accuracy. Many reports on such results are available in the literature [2]. More recent work using these models demonstrated agreement with experimental results from InP Gunn devices at higher millimeter-wave frequencies of, for example, 128 GHz in the fundamental mode [27] and 188 GHz in a second-harmonic mode [28].

The MCHB program that generated the performance predictions of Fig. 8 was developed during the studies of D-band Gunn devices in the fundamental mode [5]. To gain confidence in its predictions at high millimeter- and submillimeter-wave frequencies, the results from this program were first compared with experimental data at lower millimeter-wave frequencies, in particular at W-band [29]. Provided the material parameters that are needed for the Monte Carlo method are selected properly, very good agreement between simulation and experiment is achieved under dc and RF conditions.

Subsequently, this program was expanded to account for heat flow in the device and to include the harmonic-balance technique for devices not only operating in the fundamental mode, but also in a higher harmonic mode [8], [17]. Similar to the findings from hydrodynamic or energy-momentum models [27], excellent agreement was found with the same aforementioned experimental results at 130 and 188 GHz [17]. Compared to hydrodynamic or energy-momentum models, however, the Monte Carlo approach takes the transport dynamics of individual quasiparticles, which are subject to internal and external forces and to various scattering mechanisms, more accurately into account. In hydrodynamic models, the effect of all scattering phenomena is represented by a few relaxation-time parameters that depend on the average electron energy. Therefore, some of the highly relevant physical processes are no longer represented in the model. In particular, the Gunn effect strongly depends on scattering processes between various conduction band valleys. Therefore, they need to be taken into account accurately, especially at the high frequencies of interest in this paper.

The doping profile of Fig. 2(b) for the Gunn devices of Figs. 3 and 5 was chosen as a compromise to accommodate two different operating conditions: excellent RF performance from devices on diamond heat sinks, as well as safe operating temperatures in the active region of devices even on integral heat sinks. In addition, the studies of second-harmonic power extraction from InP Gunn devices, but also GaAs TUNNETT diodes [30], [31] indicated that the oscillator circuit imposes a different impedance limit on devices operating in a second-harmonic mode and that, therefore, areas smaller than those of devices operating in the fundamental mode must be chosen.

The thermal resistance of mesa-type devices of diameter d changes approximately with $1/d$ [32], whereas the dissipated power changes approximately with d^2. Therefore, smaller devices tend to dissipate heat better into the heat sink. Better heat dissipation allows for a wider range of doping levels in the design. Different doping profiles result in different domain-forming regions in the active region of a Gunn device. These regions, in turn, critically affect the harmonic content in the terminal current and voltage waveforms. As a consequence, much higher RF power levels are predicted for devices where the doping profiles have been optimized for second-harmonic power extraction and where safe active layer temperatures are not exceeded, as on diamond heat sinks.

A. Devices With Graded Doping Profiles

Theoretical considerations and experimental results have established already that Gunn devices with linearly graded doping profiles yield superior performance compared to devices with a uniform doping. This improvement is attributed to the enhanced electric field near the cathode and the corresponding faster transfer of electrons to higher energy valleys [5]. The doping profile of Fig. 2(c) is the result of a design optimization with a target second-harmonic frequency of 240 GHz.

Subsequent simulations were carried out to determine the potential of generating substantial RF output power levels with Gunn devices at even higher submillimeter-wave frequencies. In these simulations, the length and the doping profile of the device were varied systematically and a maximum active-layer temperature of 420 K was assumed. RF oscillations were predicted up to 500 GHz and three different designs yielded RF

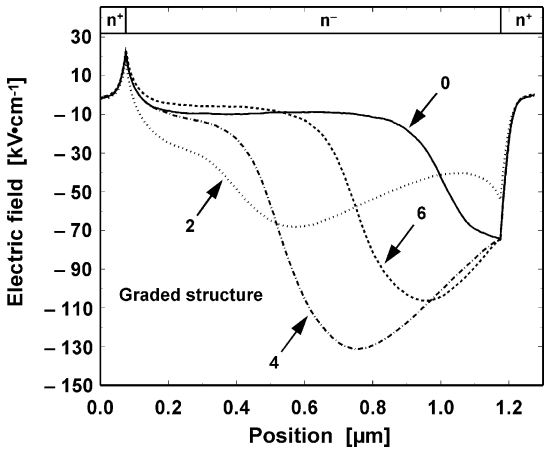

Fig. 11. Electric-field profile across Gunn device structure with the graded doping profile of Fig. 1(c) at an applied dc-bias voltage of 5 V. The different curves correspond to the instants $\omega t = n(\pi/4)$, $n = 0, 2, 4$, and 6 in one RF period.

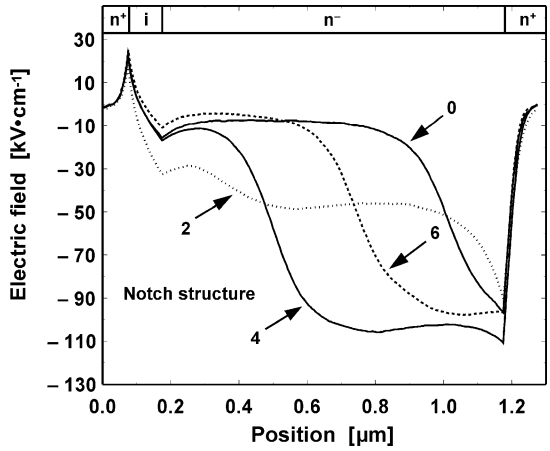

Fig. 12. Electric-field profile across a Gunn device structure with the notch doping profile of Fig. 1(d) at an applied dc-bias voltage of 5 V. The different curves correspond to the instants $\omega t = n(\pi/4)$, $n = 0, 2, 4$, and 6 in one RF period.

output power levels (and corresponding dc-to-RF conversion efficiencies) of 9.3 (1.1%), 4.8 (0.3%), and 2.6 mW (0.25%) at optimum second-harmonic frequencies of 360, 450, and 500 GHz, respectively.

B. Devices With a Notch in the Doping Profile

More complex doping profiles were considered for further improvement in RF performance at submillimeter-wave frequencies. Simulation results identified a structure with a doping notch at the cathode as the most promising candidate. This doping notch is a thin undoped epitaxial layer between the heavily n-type doped cathode contact region and the uniformly n-type doped active region, as shown in the example of Fig. 2(d). The much higher doping levels of the contact and active regions result in excess electrons in the notch region. The negative charge from these electrons causes two effects that enhance the power generating properties of the Gunn device. These two effects are a steep increase in the electric field right from the cathode contact region and a lower peak electric field profile throughout the active region. Figs. 11 and 12 illustrate the evolution of the electric-field profiles in the device at four instants of the RF cycle for the graded and notch structures, respectively. Fig. 12 clearly shows a local peak in the absolute value of the electric field at the end of the notch region. Such an increase in the electric field causes electrons to be transferred faster to the upper conduction band valleys once they are injected from the cathode, and this faster transfer corresponds to a shorter so-called "dead zone." Figs. 11 and 12 indicate that the peak electric field is reduced from more than 130 kV/cm in the graded structure to less than 110 kV/cm in the notch structure. They also reveal a flatter electric-field profile throughout the active region of the notch structure. A shorter "dead zone," a lower peak electric field, and a flatter field profile result in a more efficient Gunn effect.

The example of Fig. 2(d) was designed for approximately the same operating frequencies as the graded doping profile of Fig. 2(c). Fig. 13 compares the predicted output power levels from devices with the two structures, as shown in Fig. 2(c) and (d). The simulations were carried out at seven or eight frequency

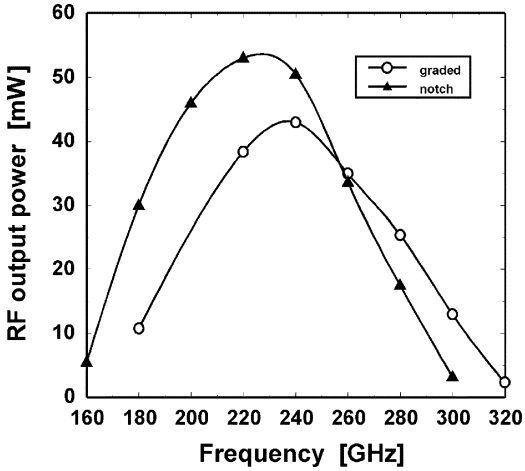

Fig. 13. Comparison of predicted RF output power levels from InP Gunn devices with the graded structure of Fig. 2(c) and the notch structure of Fig. 2(d).

points between 160–320 GHz, and based on nearly the same low active-layer temperatures for long-term reliability. The devices with the notch structure generate higher output power levels up to approximately 260 GHz. At 240 GHz, a device with the notch structure yields more than 50 mW compared to 43 mW from a device with the graded structure.

A reduction of the "dead zone" is expected to enhance the performance particularly at very high frequencies. In addition, a rather flat electric-field profile improves dc-to-RF conversion efficiencies and a lower peak electric field in the active region results in a more reliable operation of these devices. As a matter of fact, initial experimental results around 300 GHz from devices with the notch structure of Fig. 1(d) are quite promising, but comprehensive experimental evaluation of different notch structures is required to establish the favorable performance predictions, which is beyond the scope of this paper. Table I compares the predicted RF output power levels and dc-to-RF conversion efficiencies for devices with graded and notch structures at four frequencies, i.e., 240, 360, 450, and 500 GHz. These simulations assumed that all devices were mounted on diamond heat

TABLE I
COMPARISON OF THE RF SIMULATION RESULTS FOR InP GUNN DEVICES WITH GRADED AND NOTCH STRUCTURES. (ALL NOTCH STRUCTURES HAVE A 0.1-μm-LONG UNDOPED LAYER BETWEEN THE HEAVILY n-DOPED CATHODE CONTACT LAYER AND THE ACTIVE REGION. L, N_{cathode}, N_{anode}, V_{dc}, f_o, P_{RF}, AND η DENOTE LENGTH OF THE ACTIVE REGION, DOPING NEAR THE CATHODE, DOPING NEAR THE ANODE, APPLIED dc VOLTAGE, OPERATING FREQUENCY, RF OUTPUT POWER, AND dc-TO-RF CONVERSION EFFICIENCY, RESPECTIVELY)

Device Structure	L [μm]	N_{cathode} [cm^{-3}]	N_{anode} [cm^{-3}]	V_{dc} [V]	f_o [GHz]	P_{RF} [mW]	η [%]
Graded	1.1	1.0×10^{16}	3.0×10^{16}	5.0	240	43	1.1
	0.75	0.9×10^{16}	5.7×10^{16}	3.7	360	9.3	0.6
	0.65	0.9×10^{16}	1.1×10^{17}	2.9	450	4.8	0.3
	0.6	0.9×10^{16}	1.1×10^{17}	2.9	500	2.6	0.25
Notch	1.0	2.3×10^{16}	2.3×10^{16}	5.0	240	50	1.2
	0.7	4.0×10^{16}	4.0×10^{16}	3.5	360	12	0.75
	0.6	4.0×10^{16}	4.0×10^{16}	3.5	400	11	0.6
	0.5	6.0×10^{16}	6.0×10^{16}	3.0	450	8.0	0.5
	0.4	8.0×10^{16}	8.0×10^{16}	2.9	500	4.7	0.4

sinks. In addition, the maximum operating temperatures were kept below 420 K to ensure reliable long-term operation of fabricated devices.

The average doping levels in the active regions of the graded and notch structures differ by less than 20%. However, the addition of a thin notch layer significantly changes the properties of the Gunn effect in the device, as illustrated by the electric-field profiles of Figs. 11 and 12. Table I indicates that, at 240 GHz, the performance of the notch structure is slightly better than that of the graded structure with a 17% increase in RF output power. More importantly, the results in this table clearly show that the advantage of using notch structures is more pronounced at higher frequencies. In particular, at 500 GHz, the predicted output RF power from a notch structure is more than 80% higher than that of an optimized graded structure.

The effects of the so-called "dead zone" in a Gunn device need to be considered to explain the improvements. This dead zone occurs right at the cathode where most electrons are in the lowest conduction-band valley. Therefore, this region is inactive and does not contribute to the power generation in the device. It corresponds to a positive resistance, which reduces or even eliminates the negative differential resistance of the device. In devices with a doping notch, the dead zone is more effectively reduced compared to devices with a graded doping profile. In both devices, the electric field initially is small right at the cathode; however, the doping notch causes the field to rise more rapidly over a shorter distance, which corresponds to a smaller dead zone. The total length of the active region shrinks with operating frequency and, therefore, any dead zone occupies a larger fraction of it. Consequently, any reduction of the dead zone more effectively improves the RF performance the higher the operating frequency.

IV. CONCLUSION

InP Gunn device structures with a grading in the doping profile have been investigated theoretically and experimentally for their potential as fundamental solid-state sources in the frequency range of 220–500 GHz. By optimizing the doping profile in the active region, significant RF power levels were generated up to at least 328 GHz. RF power levels (and corresponding dc-to-RF conversion efficiencies) of more than 3.5 mW (0.32%) around 300 GHz and more than 2 mW around 315 GHz confirm the expected improvements from doping profile optimization. These results also represent the most powerful fundamental solid-state RF sources operated at room temperature. Additional simulation work identified a significant performance advantage in structures with a doping notch. This advantage increases with operating frequency. Both theoretical and experimental results show the strong potential of second-harmonic InP Gunn devices as compact, powerful, and reliable solid-state sources at submillimeter-wave frequencies. More theoretical and experimental work in the areas of device and RF circuit optimization is required to exploit this potential to the full extent and to establish the ultimate performance limits of InP Gunn devices and their causes.

ACKNOWLEDGMENT

The authors acknowledge the review of this paper as arranged by Editor-in-Chief M. B. Steer. The authors would like to thank P. Siegel, Jet Propulsion Laboratory, Pasadena, CA, for providing some of the most recent frequency multiplier data, K. Pruss, The University of Michigan at Ann Arbor, for machining some of the critical parts of the waveguide cavities with excellent skill, and H. Süsterhenn, Fachhochschule München, Munich, Germany, for help with electroplating those critical parts.

REFERENCES

[1] P. Siegel, "Terahertz technology," *IEEE Trans. Microwave Theory Tech.*, vol. 50, pp. 910–928, Mar. 2002.
[2] I. G. Eddison, "Indium phosphide and gallium arsenide transferred-electron devices," in *Infrared and Millimeter Waves*. Orlando, FL: Academic, 1984, vol. 11, Millimeter Components and Techniques, Part III, pp. 1–59.
[3] L. Wandinger, "mm-Wave InP Gunn devices: Status and trends," *Microwave J.*, vol. 24, no. 3, pp. 71–78, 1981.
[4] P. A. Rolland, M. R. Friscourt, D. Lippens, C. Dalle, and J. L. Nieruchalski, "Millimeter wave solid-state power sources," in *Proc. Int. Millimeter Waves Workshop*, Rome, Italy, Apr. 2–4, 1986, pp. 125–177.
[5] R. Kamoua, H. Eisele, and G. I. Haddad, "D-band (110–170 GHz) InP Gunn devices," *Solid-State Electron.*, vol. 36, pp. 1547–1555, 1993.
[6] H. Eisele and G. I. Haddad, "High-performance InP Gunn devices for fundamental-mode operation in D-band (110–170 GHz)," *IEEE Microwave Guided Wave Lett.*, vol. 5, pp. 385–387, Nov. 1995.
[7] H. Eisele, "Second-harmonic power extraction from InP Gunn devices with more than 1 mW in the 260–320 GHz frequency range," *Electron. Lett.*, vol. 34, pp. 2412–2413, 1998.
[8] R. Kamoua, "Potential of second-harmonic power generation in InP Gunn oscillators above 200 GHz," in *Proc. 4th Int. Millimeter Submillimeter Waves Applications Conf.*, San Diego, CA, July 20–24, 1998, pp. 32–37.
[9] H. Eisele and G. I. Haddad, "D-band InP Gunn devices with second-harmonic power extraction up to 290 GHz," *Electron. Lett.*, vol. 30, pp. 1950–1951, 1994.
[10] H. Eisele and R. Kamoua, "InP Gunn devices for low-noise and high-performance oscillators in the 80–400 GHz frequency range," in *Proc. IEEE 9th Int. Terahertz Electronics Conf.*, Charlottesville, VA, Oct. 15–16, 2001 [CD ROM].
[11] J. E. Carlstrom, R. L. Plambeck, and D. D. Thornton, "A continuously tunable 65–115-GHz Gunn oscillator," *IEEE Trans. Microwave Theory Tech.*, vol. MTT-33, pp. 610–619, July 1985.

[12] A. Rydberg, "High efficiency and output power from second- and third-harmonic millimeter-wave InP-TED oscillators at frequencies above 170 GHz," *IEEE Electron Device Lett.*, vol. 11, pp. 439–441, Oct. 1990.
[13] ——, "A contribution to the design of wide-band tunable second-harmonic mode millimeter-wave InP-TED oscillators above 110 GHz," *Int. J. Infrared Millim. Waves*, vol. 11, pp. 383–404, 1990.
[14] M. A. di Forte-Poisson, C. Brylinski, G. Colomer, D. Osselin, S. Hersee, J. P. Duchemin, F. Azan, D. Lechevallier, and J. Lacombe, "High-power high-efficiency LP-MOCVD InP Gunn diodes for 94 GHz," *Electron. Lett.*, vol. 20, pp. 1061–1062, 1984.
[15] H. Eisele, A. Rydberg, and G. I. Haddad, "Recent advances in the performance of InP Gunn devices and GaAs TUNNETT diodes for the 100–300-GHz frequency range and above," *IEEE Trans. Microwave Theory Tech.*, vol. 48, pp. 626–631, Apr. 2000.
[16] H. Eisele, "High performance InP Gunn devices with 34 mW at 193 GHz," *Electron. Lett.*, vol. 38, no. 16, pp. 923–924, Aug. 2002.
[17] R. Kamoua, "Monte Carlo-based harmonic balance technique for the simulation of high-frequency TED oscillators," *IEEE Trans. Microwave Theory Tech.*, vol. 46, pp. 1376–1381, Oct. 1998.
[18] H. Eisele, "Active two-terminal devices for terahertz power generation by multiplication," in *Terahertz Sources and Systems*, ser. NATO Sci. II: Math., Phys., Chem., R. E. Miles, P. Harrison, and D. Lippens, Eds., 2001, vol. 27, pp. 69–86.
[19] G. I. Haddad, J. East, and H. Eisele, "Two-terminal active devices for terahertz sources," in *Terahertz Sensing Technology*. ser. Electron. Devices Adv. Syst. Technol., D. Woolard, M. S. Shur, and W. Leorop, Eds, Singapore: World Sci., 2003, vol. I, pp. 45–77.
[20] M. Ino, T. Ishibashi, and M. Ohmori, "CW oscillation with p^+–p–n^+ silicon IMPATT diodes in 200 GHz and 300 GHz bands," *Electron. Lett.*, vol. 12, pp. 148–149, 1976.
[21] A. V. Räisäinen, "Frequency multipliers for millimeter and submillimeter wavelengths," *Proc. IEEE*, vol. 80, pp. 1842–1852, Nov. 1992.
[22] S. Verghese, K. A. McIntosh, and E. R. Brown, "Highly tunable fiber-coupled photomixers with coherent terahertz output power," *IEEE Trans. Microwave Theory Tech.*, vol. 45, pp. 1301–1309, Aug. 1997.
[23] P. G. Huggard, B. N. Ellison, P. Shen, N. J. Gomes, P. A. Davies, W. P. Shillue, A. Vaccari, and J. M. Payne, "Efficient generation of guided millimeter-wave power by photomixing," *IEEE Photon. Technol. Lett.*, vol. 14, pp. 197–199, Feb. 2002.
[24] A. Stöhr, A. Malcoci, A. Sauerwald, I. C. Mayorga, R. Güsten, and D. S. Jäger, "Ultra-wide-band traveling-wave photodetectors for photonic local oscillators," *J. Lightwave Technol.*, vol. 21, pp. 3062–3070, Dec. 2003.
[25] Y. Itoh, T. Nozokido, P. G. Huggard, B. N. Ellison, P. Shen, P. A. Davies, H. Ito, T. Ishibashi, and K. Mizuno, "Generation of short millimeter-wave radiation using dot-matrix uni-traveling-carrier photodiode," *Electron. Lett.*, vol. 39, pp. 65–67, Jan. 2003.
[26] H. Eisele, M. Naftaly, J. R. Fletcher, D. P. Steenson, and M. R. Stone, "The study of harmonic-mode operation of GaAs TUNNETT diodes and InP Gunn devices using a versatile terahertz interferometer," in *Proc. 15th Int. Space Terahertz Technology Symp.*, Northampton, MA, May 27–29, 2004.
[27] R. Judaschke, "Comparison of modulated impurity-concentration InP transferred electron devices for power generation at frequencies above 130 GHz," *IEEE Trans. Microwave Theory Tech.*, vol. 48, pp. 719–724, Apr. 2000.
[28] M. F. Zybura, S. H. Jones, G. B. Tait, and J. R. Jones, "100–300 GHz Gunn oscillator simulation through harmonic balance circuit analysis linked to a hydrodynamic device simulator," *IEEE Microwave Guided Wave Lett.*, vol. 4, pp. 282–284, Aug. 1994.
[29] R. Kamoua, H. Eisele, G. I. Haddad, G. Munns, and M. Sherwin, "Development of an appropriate model for the design of D-band InP Gunn devices," in *Proc. IEEE/Cornell Conf. Advanced Concepts in High Speed Semiconductor Devices and Circuits*, Ithaca, NY, 1993, pp. 338–346.
[30] H. Eisele, "Efficient second-harmonic power extraction from GaAs TUNNETT diodes above 200 GHz," *Electron. Lett.*, vol. 34, pp. 1324–1326, 1998.
[31] ——, "Efficient second-harmonic power extraction from GaAs TUNNETT diodes above 200 GHz," *Electron. Lett.*, vol. 34, p. 1531, 1998.
[32] L. H. Holway and M. G. Adlerstein, "Approximate formulas for the thermal resistance of IMPATT diodes compared with computer calculations," *IEEE Trans. Electron Devices*, vol. 24, pp. 156–159, 1977.

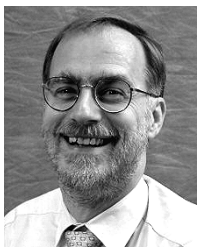

Heribert Eisele (M'98–SM'02) received the Dipl.-Ing. and Dr.-Ing. degrees from the Technical University of Munich, Munich, Germany, in 1983 and 1989, respectively, both in electrical engineering.

From 1984 to 1990, he was a Research Engineer and Teaching Assistant with the Lehrstuhl für Allgemeine Elektrotechnik und Angewandte Elektronik, Technical University of Munich, where he was involved in IMPATT diode technology, millimeter-wave measurements, and semiconductor material characterization. From 1990 to 2002, he was with the Department of Electrical Engineering and Computer Science, The University of Michigan at Ann Arbor, where he was involved with the numerical simulations and fabrication technologies of two-terminal devices, applications of two-terminal devices as power sources at millimeter- and submillimeter-wave frequencies, and optical transmission of microwave and millimeter-wave signals. In January 2003, he joined the Institute of Microwaves and Photonics, The University of Leeds, Leeds, U.K., where he is a Reader in millimeter- and submillimeter-wave electronics with the School of Electronic and Electrical Engineering. He has authored or coauthored six book chapters and over 80 technical papers in scientific journals and conference proceedings. His current research interests include solid-state devices and their applications at millimeter- and submillimeter-wave frequencies, novel semiconductor device structures and device fabrication technologies for sources of radiation in the terahertz region, and terahertz systems applications.

Dr. Eisele is a member of the Editorial Board for the IEEE TRANSACTIONS ON MICROWAVE THEORY AND TECHNIQUES.

Ridha Kamoua (S'88–M'90) received the B.S. degree in electrical engineering from the University of Rochester, Rochester, NY, in 1985, and the M.S. and Ph.D. degrees in electrical engineering from The University of Michigan at Ann Arbor, in 1987 and 1992, respectively.

In 1992, he joined the Department of Electrical and Computer Engineering, State University of New York at Stony Brook, where he is currently an Associate Professor and the Undergraduate Program Director. His research interests include development of computer models for high-frequency millimeter- and submillimeter-wave devices, design and modeling of high-performance Gunn oscillators, investigation of novel semiconductor sources for the terahertz region, and biomedical sensors.

Dr. Kamoua is a member of Eta Kappa Nu.